RESEARCH ARTICLE • OPEN ACCESS

The Effectiveness of B Cells in CAR T Cell Therapy for B Cells Acute Lymphoblastic Leukemia

Elena M. D. P. Haries and Abadi Abadi

Volume 6, Issue 3, Pages 252–261, September 2025

Received 9 June 2025, Revised 17 August 2025, Accepted 16 September 2025, Published Online 30 September 2025

To Cite this Article : E. M. D. P. Haries and A. Abadi,"The Effectiveness of B Cells in CAR T Cell Therapy for B Cells Acute Lymphoblastic Leukemia", *Jambura J. Biomath*, vol. 6, no. 3, pp. 252–261, 2025, *https://doi.org/10.37905/jjbm.v6i3.32511*

JOURNAL INFO • JAMBURA JOURNAL OF BIOMATHEMATICS

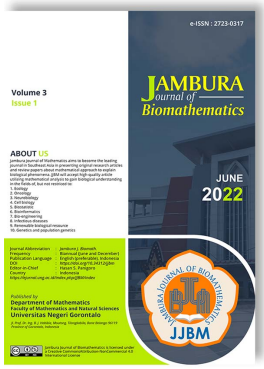

Homepage	:	http://ejurnal.ung.ac.id/index.php/JJBM/index
Journal Abbreviation	:	Jambura J. Biomath.
Frequency	:	Quarterly (March, June, September and December)
Publication Language	:	English
DOI	:	https://doi.org/10.37905/jjbm
Online ISSN	:	2723-0317
Editor-in-Chief	:	Hasan S. Panigoro
Publisher	:	Department of Mathematics, Universitas Negeri Gorontalo
Country	:	Indonesia
OAI Address	:	http://ejurnal.ung.ac.id/index.php/jjbm/oai
Google Scholar ID	:	XzYgeKQAAAAJ
Email	:	editorial.jjbm@ung.ac.id

JAMBURA JOURNAL • FIND OUR OTHER JOURNALS

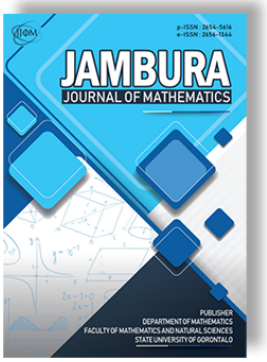

Jambura Journal of Mathematics

Jambura Journal of Mathematics Education

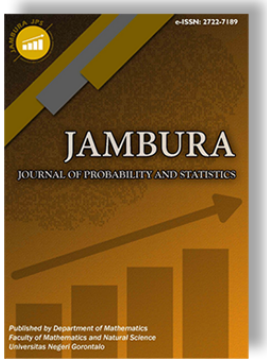

Jambura Journal of Probability and Statistics

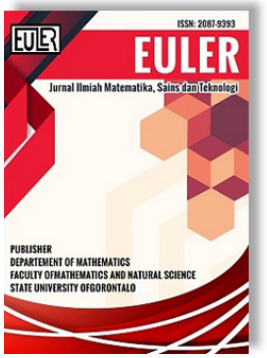

EULER : Jurnal Ilmiah Matematika, Sains, dan Teknologi

Jambura Journal of Biomathematics, Volume 6, Issue 3, Pages 252–261, September 2025 https://doi.org/10.37905/jjbm.v6i3.32511

Research Article

Check for updates

The Effectiveness of B Cells in CAR T Cell Therapy for B Cells Acute Lymphoblastic Leukemia

Elena M. D. P. Haries[1] **and Abadi Abadi**[1,*]

[1]*Department of Mathematics, Faculty of Mathematics and Natural Sciences, Universitas Negeri Surabaya, Surabaya 60213, Indonesia*

ARTICLE HISTORY
Received 9 June 2025
Revised 17 August 2025
Accepted 16 September 2025
Published 30 September 2025

KEYWORDS
Leukemia
B cell
CAR T cell therapy
Stability analysis
Bifurcation

ABSTRACT. *Chimeric Antigen Receptor (CAR) T cell therapy has shown remarkable clinical outcomes in B cell Acute Lymphoblastic Leukemia (B-ALL). The treatment can utilize the immune system to recognize and kill leukemia cells through the CD19 antigen target. However, the CD19 antigen is also expressed on normal B cells, which can cause side effects in B cell aplasia. This study modifies a mathematical model of the interaction between CAR T cells, leukemia cells, and normal B cells by introducing the assumption that leukemia cells follow logistic growth dynamics. Determined the equilibrium point and continues to analyze stability using linearization and the Routh-Hurwitz criterion. The analysis reveals four equilibrium points, including a state where leukemia cells grow at maximum capacity in the absence of CAR T cells. Bifurcation analysis shows the occurrence of both transcritical and subcritical Hopf bifurcations, with distinct patterns compared to previous models. A heteroclinic cycle was also identified, indicating that relapse may occur even after remission. The logistic growth and B cell progenitors not only shape remission and relapse dynamics but also explain the dual role of B cells in sustaining CAR T activation and causing complications such as Cytokine Release Syndrome (CRS). This provides new insights for understanding therapy outcomes and optimizing CAR T cell treatment strategies.*

1. Introduction

Epidemiological data shows that leukemia accounts for approximately 2.5% of the total incidence of all cancers and 3.1% of the mortality of all cancers worldwide in 2020 [1]. Based on the American Cancer Society 2024 [2], the estimated new cases of leukemia are 33% (62,770 cases). The number of cases makes leukemia one of the deadliest diseases.

Leukemia is a type of blood cancer that occurs due to the production of abnormal white blood cells in the bone marrow [3–5]. Blood is essential in the human body because it transports the oxygen, nutrients, and hormones necessary for survival. Blood consists of blood plasma, white blood cells, red blood cells, and platelets, all of which play essential roles in maintaining the body's health. If the blood is impaired, it can cause the body to function incorrectly, and various organ systems will be disrupted. Blood disorders can affect the various working systems of white blood cells, red blood cells, and plasma. Leukemia cells are one of the disorders that can disrupt blood cells, as when the number of leukemia cells increases, they enter the bloodstream and spread to other organs from the bone marrow. In its early stages, leukemia often causes no signs. Symptoms typically appear only when cancer cells have progressed and begun to invade and damage the body's cells. In general, symptoms that occur in people with leukemia include fever, drastic weight loss, anemia, red spots on the skin, nosebleeds, easy bruising, swollen lymph nodes, and abdominal discomfort [6, 7].

The four major types of leukemia are acute myeloid leukemia (AML), acute lymphoblastic leukemia (ALL), chronic myeloid leukemia (CML), and chronic lymphocytic leukemia (CLL). Myeloid and lymphoid denote the involvement of these cell types in the disease, whereby lymphoid cells include B and T lymphocytes, as well as innate lymphoid cells, and myeloid cells comprise the rest of the blood and immune cells that arise from the hematopoietic stem cell (HSC). Acute and chronic denote whether the malignant cells proliferate or more slowly [8]. ALL is most common in childhood and adolescence, accounts for approximately 75% of all leukemia cases in individuals under 20 years of age and approximately one-quarter of all pediatric cancers. The peak incidence is in children ages 2–5 years [9]. In ALL, the precursor lymphoid neoplasms are broadly categorized based on their lineage into B-lymphoblastic leukemia (B-ALL) and T-lymphoblastic leukemia (T-ALL) [10–12]. 85% of ALL cases are caused by the B-LLA type [13].

One of the immunotherapy treatments for B-ALL is CAR T (Chimeric Antigen Receptor T) cell therapy. It is a therapy that consists of genetically modifying T cells to recognize specific cancer cell antigens [14]. This therapy utilizes CD8 T lymphocytes or cytotoxic cells to fight cancer by modifying the surface antigen receptors of the patient's CD8 cells ex vivo. Before modifying antigen receptors on CD8 cells, cancer cells often practiced resistance in order not to be detected by CD8 cells so that cancer cells could continue to multiply. After genetic modification, CAR T cells will be infused back into the patient. Furthermore, these CAR T cells target cancer cell surface antigens, especially

*Corresponding Author.

Email : *abadi@unesa.ac.id* (A. Abadi)
Homepage : http://ejurnal.ung.ac.id/index.php/JJBM/index / E-ISSN : 2723-0317

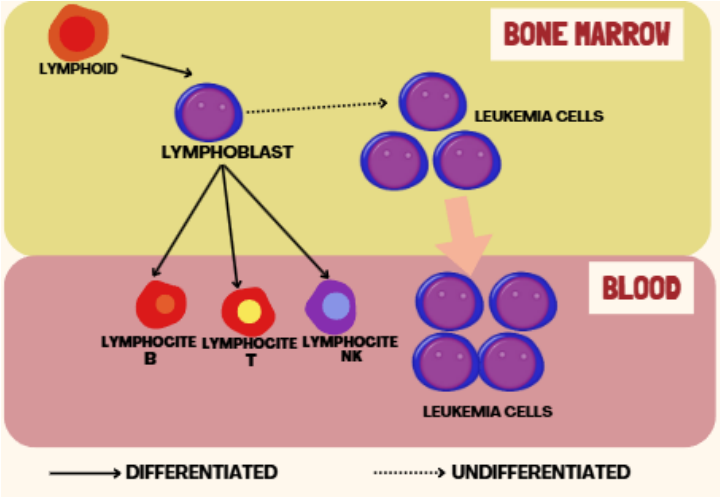

Figure 1. Dynamics of leukemia cells, CAR T cells, and B cells in the blood

the CD19 antigen. CD19 antigen is usually expressed in B-ALL [10]. Based on Ghorashian, Pule, and Amrolia, as cited in [15], who reported that approximately 90% of CAR T cell therapies have demonstrated remarkable anti-tumor efficacy against B cell malignancies, particularly acute lymphoblastic leukemia (ALL).

Although this therapy has shown success, there are a number of treatment-related toxicities such as cytokine release syndrome (CRS) [16]. CRS is a systemic disorder characterized by nausea, headache, tachycardia, fever, hypotension, rash, and shortness of breath, caused by a rapid release of cytokines from cells [15]. CRS occurs when the immune system responds more aggressively to infection or immunotherapy drugs than it should. This condition occurs due to the action of CAR T cells against the leukemia cell antigen CD19. Another less described side effect is the occurrence of aplasia or a condition characterized by a very low number of B cells [17]. This condition occurs when CAR T cells attack and kill leukemia cells with the CD19 antigen and B cells are also attacked. CD19 antigen is expressed in every phase of B cells [15]. In fact, B cells in peripheral blood serve as a surrogate marker for CAR T persistence, and the loss of B cells is associated with a higher likelihood of disease recurrence. This is because new B cells are continuously produced in the bone marrow, providing an endless source of stimulation for the CAR T cell population and acting as an endogenous vaccine [18]. The phenomena that occur can be described Figure 1.

Mathematical modeling provides a useful tool to study the interactions between leukemia cells, CAR T cells, and B cells. Previous models, such as Serrano et al. [19], assumed exponential growth of leukemia cells and did not include time-series simulations, which limits their ability to capture realistic clinical scenarios. In reality, leukemia cells grow under resource constraints, following logistic dynamics [18].

To address this limitation, this study modifies the previous model by incorporating logistic growth of leukemia cells and performing time-series simulations to examine remission, relapse, and coexistence. We hypothesize that this extended model can better represent CAR T therapy dynamics and capture outcomes observed in clinical practice. The objectives of this study are: (1) to develop the extended model, (2) to analyze equilibria and bifurcations, (3) to perform numerical simulations, and (4) to compare the results with earlier models to highlight new biological insights, including potential CRS occurrence.

2. Mathematical Model

This study reconstructs the mathematical model of Serrano et al. [19] assuming that the population of leukemia cells grows logistically [18]. The mathematical model consists of three populations, that is, the CAR T cell population (C), the leukemia cell population (L), and the B cell population (B). The assumptions used in this study are: (i) the type of leukemia in this study is B-Acute Lymphoblastic Leukemia (B-ALL); (ii) individuals affected by Acute Lymphoblastic B-Leukemia have been given chemotherapy before and can perform CAR T cell therapy treatment; (iii) CAR T cells have been infused into the patient's blood; (iv) this study only involved B cells, leukemia cells, and CAR T cells; (v) leukemia cells and B cells are assumed to express the CD19 antigen. These assumptions are biologically reasonable because both B cells and leukemia cells express the CD19 antigen, which is the direct target of CAR T cells [20]. The logistic growth of leukemia cells reflects the fact that their proliferation is rapid at early stages but eventually limited by resource competition and the bone marrow microenvironment [21]. Furthermore, focusing only on CAR T cells, B cells, and leukemia cells captures the dominant interactions relevant to CD19 targeted CAR T cell therapy, while the contribution of other immune populations is comparatively minor in shaping treatment dynamics. Hence, the mathematical model under study is as follows.

$$\begin{aligned}
\frac{dC}{dt} &= C\left(\rho_C(L+B+I_0) - \frac{1}{\tau_C}\right),\\
\frac{dL}{dt} &= \rho_L L\left(1 - \frac{L}{L_{\max}}\right) - \alpha C L,\\
\frac{dB}{dt} &= \frac{I_0}{\tau_{I_0}} - B\left(\alpha C + \frac{1}{\tau_B}\right),
\end{aligned} \tag{1}$$

where ρ_C represents the level of mitotic stimulation resulting from interactions with CD19 cells distributed throughout the body. ρ_L denotes the proliferation rate of leukemia cells, while $L_{\max}$ indicates the carrying capacity for leukemia cells. The parameter α quantifies the probability of interaction between CAR

T cells and CD19 cells. Additionally, τ_C and τ_B refer to the average lifespans of CAR T cells and B cells, respectively, while I_0 represents the total number of B cells produced during B cell development. Lastly, τ_{I_0} symbolizes the average lifespan of B cell progenitors. All parameters and constants in the system are positive.

3. Equilibria of The System

The equilibria of system (1) are obtained by taking $\frac{dC}{dt} = \frac{dL}{dt} = \frac{dB}{dt} = 0$. In this study, we have four equilibria:

1. $P_1\left(0, 0, \frac{I_0\tau_B}{\tau_{I_0}}\right)$
   The condition that CAR T cells effectively eliminate leukemia cells, but they also have a limited lifespan and eventually die themselves. On the other hand, B cells typically thrive and increase in number, with progenitor B cells having an average lifespan of τ_B.
2. $P_2\left(0, L_{\max}, \frac{I_0\tau_B}{\tau_{I_0}}\right)$
   The condition in which leukemia cells grow maximally without therapy.
3. $P_3\left(\frac{1}{\alpha}\left(\frac{I_0}{\tau_{I_0}\left(\frac{1}{\rho_C\tau_C} - I_0\right)} - \frac{1}{\tau_B}\right), 0, \frac{1}{\rho_C\tau_C} - I_0\right)$
   The state of CAR T cell therapy has been utilized to eliminate leukemia cells, leading to the stimulation of B cells so that CAR T cells can survive. The equilibrium point P_3 exists when $I_0 \in \left(\frac{1}{\rho_C\tau_C}\left(1 - \frac{\tau_B}{\tau_B+\tau_{I_0}}\right), \frac{1}{\rho_C\tau_C}\right)$.
4. $P_4(C^*, L^*, B^*)$ with

$$C^* = \frac{1}{2\alpha}\left(-\frac{A}{\tau_{I_0}L_{\max}} + D\right), \tag{2}$$

$$L^* = L_{\max}\left(1 - \frac{1}{2\rho_L}\left(-\frac{A}{\tau_{I_0}L_{\max}} + D\right)\right), \tag{3}$$

$$B^* = \frac{1}{\rho_C\tau_C} - L_{\max}\left(1 - \frac{1}{2\rho_L}\left(-\frac{A}{\tau_{I_0}L_{\max}} + D\right)\right) - I_0, \tag{4}$$

where

$$\Delta = \frac{1}{\rho_C\tau_C} - L_{\max} - I_0,$$

$$A = \frac{\tau_{I_0}L_{\max}}{\tau_B} + \rho_L\tau_{I_0}\Delta,$$

$$D = \sqrt{\left(\frac{\tau_{I_0}L_{\max}}{\tau_B}\right)^2 + (\rho_L\tau_{I_0}\Delta)^2 + \frac{4\rho_L}{L_{\max}}\left(\frac{\Delta}{\tau_B} - \frac{I_0}{\tau_{I_0}}\right)}.$$

The equilibrium point P_4 refers to the condition where leukemia cells, CAR T cells, and B cells coexist.

4. Stability Analysis

The system of eq. (1) is a system of nonlinear differential equations. Therefore, the stability analysis is performed using linearization. Linearize the system to obtain the Jacobian matrix as follows:

$$J = \begin{bmatrix} J_{11} & J_{12} & J_{13} \\ J_{21} & J_{22} & J_{23} \\ J_{31} & J_{32} & J_{33} \end{bmatrix}, \tag{5}$$

where

$$J_{11} = \rho_C(L + B + I_0) - \frac{1}{\tau_C}, \quad J_{12} = \rho_C C,$$
$$J_{13} = \rho_C C, \qquad J_{21} = -\alpha L,$$
$$J_{22} = \rho_L - \frac{2\rho_L L}{L_{\max}} - \alpha C, \qquad J_{23} = 0,$$
$$J_{31} = -\alpha B, \qquad J_{32} = 0,$$
$$J_{33} = -\alpha C - \frac{1}{\tau_B}.$$

Utilizing the Jacobian matrix eq. (5), we analyze the stability of each equilibrium point of the system from its eigenvalues.

4.1. Equilibrium Point $P_1\left(0, 0, \frac{I_0\tau_B}{\tau_{I_0}}\right)$

Theorem 1. *The equilibrium point $P_1\left(0, 0, \frac{I_0\tau_B}{\tau_{I_0}}\right)$ is a saddle point and unstable.*

Proof. By substituting the equilibrium point $P_1(0, 0, \frac{I_0\tau_B}{\tau_{I_0}})$ into the Jacobian matrix eq. (5), we obtain:

$$J(P_1) = \begin{bmatrix} \rho_C\left(\frac{I_0\tau_B}{\tau_{I_0}} + I_0\right) - \frac{1}{\tau_C} & 0 & 0 \\ 0 & \rho_L & 0 \\ -\frac{\alpha I_0\tau_B}{\tau_{I_0}} & 0 & -\frac{1}{\tau_B} \end{bmatrix}. \tag{6}$$

The corresponding characteristics equation for eq. (6) gives the eigenvalues: $\lambda_1 = \rho_C\left(\frac{I_0\tau_B}{\tau_{I_0}} + I_0\right) - \frac{1}{\tau_C}, \lambda_2 = \rho_L, \lambda_3 = -\frac{1}{\tau_B}$. Since $\rho_L > 0$, the equilibrium point $P_1$is a saddle point and unstable. □

4.2. Equilibrium Point $P_2\left(0, L_{\max}, \frac{I_0\tau_B}{\tau_{I_0}}\right)$

Theorem 2. *The equilibrium point $P_2\left(0, L_{\max}, \frac{I_0\tau_B}{\tau_{I_0}}\right)$ is an locally asymptotically stable node if*

$$I_0 < \left(\frac{1}{\rho_C\tau_C} - L_{\max}\right)\left(1 - \frac{\tau_B}{\tau_B + \tau_{I_0}}\right).$$

Proof. By substituting the equilibrium point $P_2\left(0, L_{\max}, \frac{I_0\tau_B}{\tau_{I_0}}\right)$ into the Jacobian matrix eq. (5), we obtained:

$$J(P_2) = \begin{bmatrix} \rho_C\left(L_{\max} + \frac{I_0\tau_B}{\tau_{I_0}} + I_0\right) - \frac{1}{\tau_C} & 0 & 0 \\ -\alpha L_{\max} & -\rho_L & 0 \\ -\frac{\alpha I_0\tau_B}{\tau_{I_0}} & 0 & -\frac{1}{\tau_B} \end{bmatrix}. \tag{7}$$

The corresponding characteristics equation for eq. (7) gives the eigenvalues:

$$\lambda_1 = \rho_C\left(L_{\max} + \frac{I_0\tau_B}{\tau_{I_0}} + I_0\right) - \frac{1}{\tau_C},$$
$$\lambda_2 = -\rho_L,$$
$$\lambda_3 = -\frac{1}{\tau_B}.$$

Since $I_0 < \left(\frac{1}{\rho_C \tau_C} - L_{\max}\right)\left(1 - \frac{\tau_B}{\tau_B + \tau_{I_0}}\right)$, then $\lambda_1 < 0$. Therefore, the equilibrium point P_2 is an asymptotically stable node. □

4.3. Equilibrium Point

$P_3\left(\frac{1}{\alpha}\left(\frac{I_0}{\tau_{I_0}\left(\frac{1}{\rho_C\tau_C} - I_0\right)} - \frac{1}{\tau_B}\right), 0, \frac{1}{\rho_C\tau_C} - I_0\right)$

Theorem 3. *The equilibrium point P_3 is a spiral point and locally asymptotically stable if*

$$I_0 \in \left(\frac{1}{\rho_C\tau_C}\left(1 - \frac{\tau_B}{\tau_B + \tau_{I_0}(1 + \tau_B\rho_L)}\right), \frac{1}{\rho_C\tau_C}\right).$$

Proof. By substituting the equilibrium point P_3 into the Jacobian matrix eq. (5), we obtained:

$$J(P_3) = \begin{bmatrix} 0 & a_{12} & a_{13} \\ 0 & a_{22} & 0 \\ a_{31} & 0 & a_{33} \end{bmatrix}. \tag{8}$$

where

$$\begin{aligned}
a_{12} &= \frac{\rho_C}{\alpha}\left(\frac{I_0}{\tau_{I_0}\left(\frac{1}{\rho_C\tau_C} - I_0\right)} - \frac{1}{\tau_B}\right), \\
a_{13} &= \frac{\rho_C}{\alpha}\left(\frac{I_0}{\tau_{I_0}\left(\frac{1}{\rho_C\tau_C} - I_0\right)} - \frac{1}{\tau_B}\right), \\
a_{22} &= \rho_L - \frac{I_0}{\tau_{I_0}\left(\frac{1}{\rho_C\tau_C} - I_0\right)} + \frac{1}{\tau_B}, \\
a_{31} &= -\left(\frac{I_0}{\tau_{I_0}\left(\frac{1}{\rho_C\tau_C} - I_0\right)} - \frac{1}{\tau_B}\right) - \frac{1}{\tau_B}, \\
a_{33} &= \frac{I_0}{\tau_{I_0}\left(\frac{1}{\rho_C\tau_C} - I_0\right)}.
\end{aligned}$$

The corresponding characteristics equation for eq. (8) gives the eigenvalues:

$$\begin{aligned}
\lambda_1 &= \rho_L - \frac{I_0}{\tau_{I_0}\left(\frac{1}{\rho_C\tau_C} - I_0\right)} + \frac{1}{\tau_B}, \\
\lambda_{2,3} &= \frac{1}{2}\left(a_{33} \pm \sqrt{(-a_{33})^2 - 4\alpha a_{12}\left(\frac{1}{\rho_C\tau_C} - I_0\right)}\right).
\end{aligned}$$

Since $I_0 > \frac{1}{\rho_C\tau_C}\left(1 - \frac{\tau_B}{\tau_B + \tau_{I_0}(1+\tau_B\rho_L)}\right)$, then $\lambda_1 < 0$. Since $I_0 < \frac{1}{\rho_C\tau_C}$, then $\lambda_{2,3} \in \mathbb{C}$ with $Re(\lambda_{2,3}) < 0$. Therefore, the equilibrium point P_3 is an asymptotically stable spiral. □

4.4. Equilibrium Point $P_4(C^*, L^*, B^*)$

Theorem 4. *The equilibrium point $P_4(C^*, L^*, B^*)$ is locally asymptotically stable if*

1. $p_1 > 0$,
2. $p_1p_2 - p_3 > 0$, *and*
3. $p_3 > 0$

where

$$p_1 = -\operatorname{tr}(J(P_4)), \quad p_2 = \sum_{i=1}^{3} M_{ii}, \quad p_3 = -\det(J(P_4)),$$

with M_{ii} denotes the 2×2 principal minor of $J(P_4)$.

Proof. By substituting the equilibrium point P_4 into the Jacobian matrix eq. (5), we obtained:

$$J(P_4) = \begin{bmatrix} b_{11} & b_{12} & b_{13} \\ b_{21} & b_{22} & 0 \\ b_{31} & 0 & b_{33} \end{bmatrix}, \tag{9}$$

where coefficient of b_{ij} are defined according to the system parameters. The corresponding characteristics equation for eq. (9) is given by:

$$p_0\lambda^3 + p_1\lambda^2 + p_2\lambda + p_3 = 0. \tag{10}$$

with

$$\begin{aligned}
p_0 &= 1, \\
p_1 &= -(b_{11} + b_{22} + b_{33}) \\
&= -\operatorname{tr}(J(P_4)), \\
p_2 &= b_{11}b_{22} + b_{11}b_{33} + b_{22}b_{33} - b_{13}b_{31} - b_{12}b_{21} \\
&= \sum_{i=1}^{3} M_{ii}, \\
p_3 &= -b_{11}b_{22}b_{33} + b_{31}b_{22}b_{13} + b_{33}b_{21}b_{12} \\
&= -\det(J(P_4)),
\end{aligned}$$

where M_{ii} principal minor of $J(P_4)$. To determine the type of stability at the equilibrium point P_4, we use the following Routh's table of the characteristic equation eq. (10). Since $p_0 = 1$, the

Table 1. Routh's Table

λ^3	p_0	p_2	0
λ^2	p_1	p_3	0
λ^1	$\frac{p_1p_2 - p_3}{p_1}$	0	0
λ^0	p_3	0	0

Routh-Hurwitz Criterion says that the condition for the eigenvalues of the eq. (10) to be negative, or to have a negative real part, is that all the terms in the first column of Table 1 must be positive. In other words, the following conditions are satisfied: $p_1 > 0$, $p_1p_2 - p_3 > 0$, and $p_3 > 0$. These are conditions (i), (ii), and (iii), respectively, required. This completes the proof. □

For a more thorough analysis, exploring the global stability of the system should be considered in future studies.

5. Numerical Results

Numerical simulations were conducted using the parameter values specified in Table 2, with initial values set at $C_0 = 5 \times 10^9$, $L_0 = 7 \times 10^8$, and $B_0 = 3 \times 10^9$. In this study, we

Table 2. Values of the Parameters

Parameters	Description	Value	Source
I_0	B cell progenitor population	varies	[19]
ρ_C	Proliferation rate of CAR T cell	10^{-11}	[19]
ρ_L	Proliferation rate of leukemia cell	0.2	[19]
L_{max}	carrying capacity of leukemia cell	varies	[18]
α	Interaction rate between CAR T cells and leukemia cells	10^{-11}	[19]
τ_C	Means lifetime of CAR T cell	20	[19]
τ_{I_0}	Means lifetime of B cell progenitors	4	[19]
τ_B	Means lifetime of B cell	40	[19]

[1] I_0 represents the initial number of B cell progenitor. The different values of I_0 are selected to determine the dynamics of the effect of B cells on cancer.
[2] L_{max} denotes the carrying capacity of leukemia cells, modeled by logistic growth. Values can be selected based on a range (10^9–10^{12}) to represent different tumor spaces, with the higher value corresponding to more aggressive disease progression.

assumed the carrying capacities of leukemia cells $L_{\text{max}} = 10^9$ compared to that assumed in [18], i.e.: $L_{\text{max}} = 10^{12}$. To study the dynamics of the solutions, we implemented three different values for I_0: 10^9, 3×10^9, and 6×10^9. These are divided into the following cases.

5.1. *Case 1:* $L_{\text{max}} = 10^9$ *and* $I_0 = 10^9$

When $L_{\text{max}} = 10^9$ and $I_0 = 10^9$, we find that the equilibrium points $P_1 = (0, 0, \frac{I_0\tau_B}{\tau_{I_0}})$ and $P_2 = (0, L_{\text{max}}, \frac{I_0\tau_B}{\tau_{I_0}})$ are both saddle points and thus unstable. The equilibrium point P_3 is also unstable. In contrast, the equilibrium point P_4 is asymptotically stable, as it satisfies the conditions outlined in Theorem 4. Figure 2a illustrates that when the carrying capacity of leukemia cell, $L_{\text{max}} = 10^9$ and the initial progenitor B cell population of $I_0 = 10^9$, the equilibrium point $P_4 = (C^*, L^*, B^*)$ is asymptotically stable. This equilibrium corresponds to a coexistence state where leukemia cells, B cells, and CAR T cells persist together. Biologically, this means that although the leukemia population is not eradicated, its growth is effectively restrained by the immune response, particularly through the action of CAR T cells supported by the presence of B cells. In this state, the system reaches a balance where tumor cells remain present but at a stable and controlled level, preventing uncontrolled proliferation. Such a condition may represent a chronic but manageable disease state, in which therapy does not completely cure the leukemia but maintains it under long-term control, mimicking partial remission observed clinically.

5.2. *Case 2:* $L_{\text{max}} = 10^9$ *and* $I_0 = 3 \times 10^9$

When $L_{\text{max}} = 10^9$ and $I_0 = 3 \times 10^9$, we find that the equilibrium points $P_1 = (0, 0, \frac{I_0\tau_B}{\tau_{I_0}})$ and $P_2 = (0, L_{\text{max}}, \frac{I_0\tau_B}{\tau_{I_0}})$ are classified as a saddle point and are unstable. In contrast, the equilibrium point P_3 is asymptotically stable. Meanwhile, the equilibrium point $P_4 = (C^*, L^*, B^*)$ does not exist because there is a negative value, which is not possible for the total population. Figure 2b demonstrates that the graphs converge to the equilibrium point $P_3 = (3.5 \times 10^{10}, 0, 2 \times 10^9)$. This equilibrium is asymptotically stable, with the trajectories showing that the leukemia cell population tends toward zero, while CAR T cells and B cells remain positive. Biologically, this behavior corresponds to a complete eradication of leukemia cells by CAR T therapy. The vanishing of leukemic cells indicates that the immune-mediated killing is sufficiently strong to overcome the proliferative capacity of the tumor. At the same time, the persistence of B cells plays an important role, since they continue to provide antigenic stimulation for CAR T cells, allowing these immune effectors to expand and survive for a longer period. This dynamic interaction prevents immune exhaustion and ensures that CAR T cells remain active even after the leukemic burden has disappeared. Clinically, this scenario reflects a state of durable remission or potential cure, where the disease is eliminated and long-term immune surveillance is established. Such an outcome illustrates the therapeutic potential of CAR T therapy to achieve not only temporary control but also lasting elimination of leukemia, provided that the balance between B cell stimulation and CAR T cell persistence is maintained.

5.3. *Case 3:* $L_{\text{max}} = 10^9$ *and* $I_0 = 6 \times 10^9$

Increasing the value of $I_0 = 6 \times 10^9$, it is determined that the equilibrium points $P_1 = (0, 0, \frac{I_0\tau_B}{\tau_{I_0}})$ and $P_2 = (0, L_{\text{max}}, \frac{I_0\tau_B}{\tau_{I_0}})$ are unstable, while The equilibrium point P_3 fails to exist. Furthermore, the equilibrium point P_4 does not exist as well due to the presence of a negative population. Figure 2c illustrates that although leukemia cells can be eliminated and B cells get stimulated, CAR T cells keep growing. This does not converge to any equilibrium point. Biologically, this situation represents an unrealistic condition, since in reality CAR T cells cannot expand indefinitely in the patient's body. Such uncontrolled proliferation may be interpreted as a model representation of therapy-related toxicity, such as cytokine release syndrome (CRS), which arises from excessive immune activation. In other words, while the therapy succeeds in eradicating leukemia under this parameter setting, it may also lead to severe side effects due to the lack of regulatory mechanisms controlling CAR T cell expansion. This outcome highlights the necessity of incorporating biological feedback or regulation in the model to capture a more realistic therapeutic scenario, where leukemia eradication is achieved without dangerous immune overactivation.

5.4. *Case 4:* $L_{\text{max}} = 10^{12}$ *and* $I_0 = 10^9$

Taking when $L_{\text{max}} = 10^{12}$ and $I_0 = 10^9$, it is determined that the equilibrium points $P_1 = (0, 0, \frac{I_0\tau_B}{\tau_{I_0}})$ and $P_2 = (0, L_{\text{max}}, \frac{I_0\tau_B}{\tau_{I_0}})$ are unstable. The equilibrium point P_3 is unstable because it does not satisfy the condition of Theorem 3. In contrast, the equilibrium point $P_4 = (C^*, L^*, B^*)$ is asymptotically stable, as it meets the criteria outlined in Theorem 4. The graph

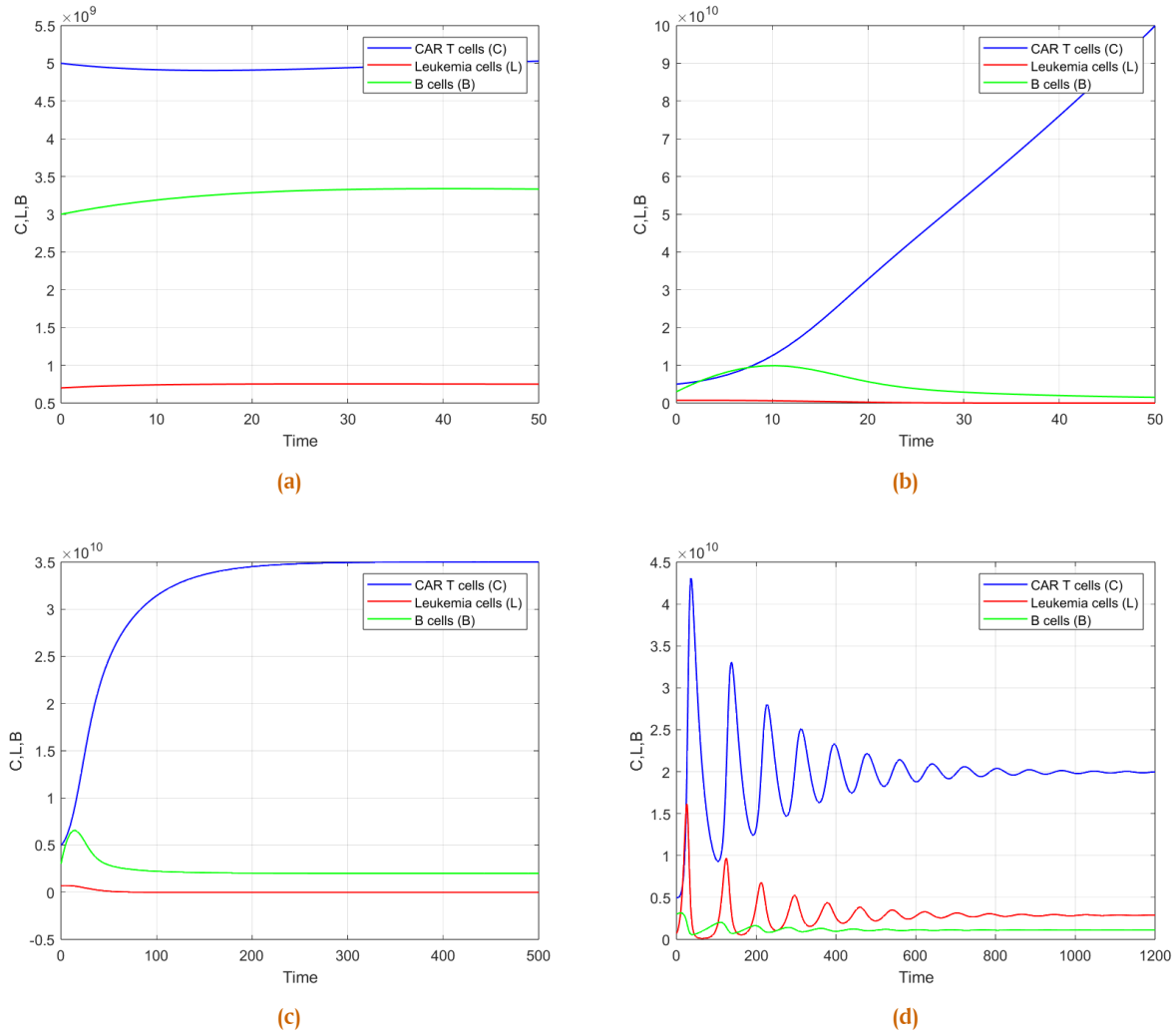

Figure 2. (a) Numerical simulation of solution of system eq. (1) when $I_0 = 10^9; L_{\max} = 10^9$. (b) Numerical simulation of solution of system eq. (1) when $I_0 = 3\times10^9; L_{\max} = 10^9$. (c) Numerical simulation of solution of system eq. (1) when $I_0 = 6\times10^9; L_{\max} = 10^9$. (d) Numerical simulation of solution of system eq. (1) when $I_0 = 10^9; L_{\max} = 10^{12}$.

in Figure 2d illustrates that when $L_{\max} = 10^{12}$ and $I_0 = 10^9$, the condition means that all three populations CAR T cells, B cells, and leukemia cells remain positive and eventually reach a stable coexistence state after initial oscillations. These oscillations represent cycles of partial remission and relapse, which biologically resemble clinical conditions where the leukemia burden temporarily decreases before stabilizing at a chronic level. This indicates that leukemia cells cannot be completely eradicated but instead persist at a stable level together with B cells and CAR T cells.

Unlike Cases 1-3 where the number of leukemia cells is the lowest (or even completely eliminated) among the other two cell populations, in Case 4 the number of leukemia cells is higher than that of B cells. For $I_0 = 3 \times 10^9$ and $I_0 = 6 \times 10^9$, the system solution will be the same as in Case 2 and Case 3. In the following simulations, we study the stability of the solutions and their bifurcations. Based on the expression of the equilibria, we divide the $I_0 - \tau_C\rho_C$ plane into regions, in which the stability of each equilibrium point is determined, as shown in Figure 3a. The graph in Figure 3a displays four distinct curves, each corresponding to the stability conditions of specific equilibrium points. The yellow curve is defined by the equation $I_0 = \left(\frac{1}{\rho_C\tau_C} - L_{\max}\right)\left(1 - \frac{\tau_B}{\tau_B+\tau_{I_0}}\right)$. The blue curve is given by $I_0 = \frac{1}{\rho_C\tau_C}\left(1 - \frac{\tau_B}{\tau_B+\tau_{I_0}}\right)$. The green curve can be expressed as $I_0 = \frac{1}{\rho_C\tau_C}\left(1 - \frac{\tau_B}{\tau_B+\tau_{I_0}(1+\tau_B\rho_L)}\right)$. Finally, the red curve is represented by: $I_0 = \frac{1}{\rho_C\tau_C}$. Additionally, the dashed black line indicates the value of $\rho_C\tau_C$, which is 2×10^{-10}. Based on these curves, five regions can be identified: R_1, R_2, R_3, R_4, and R_5.

In region R_1, that is $I_0 < \left(\frac{1}{\rho_C\tau_C} - L_{\max}\right)\left(1 - \frac{\tau_B}{\tau_B+\tau_{I_0}}\right)$. The stability of each equilibrium point is as follows:

1. The equilibrium point P_1 exists and is unstable, with a stable manifold of dimension 2 and an unstable manifold of dimension 1. Therefore, the dimensions of the manifolds at equilibrium point P_1 are given by $(\dim(W^s(P_1)), \dim(W^u(P_1))) = (2, 1)$.
2. The equilibrium point P_2 exists and is asymptotically stable. The dimensions of the stable and unstable

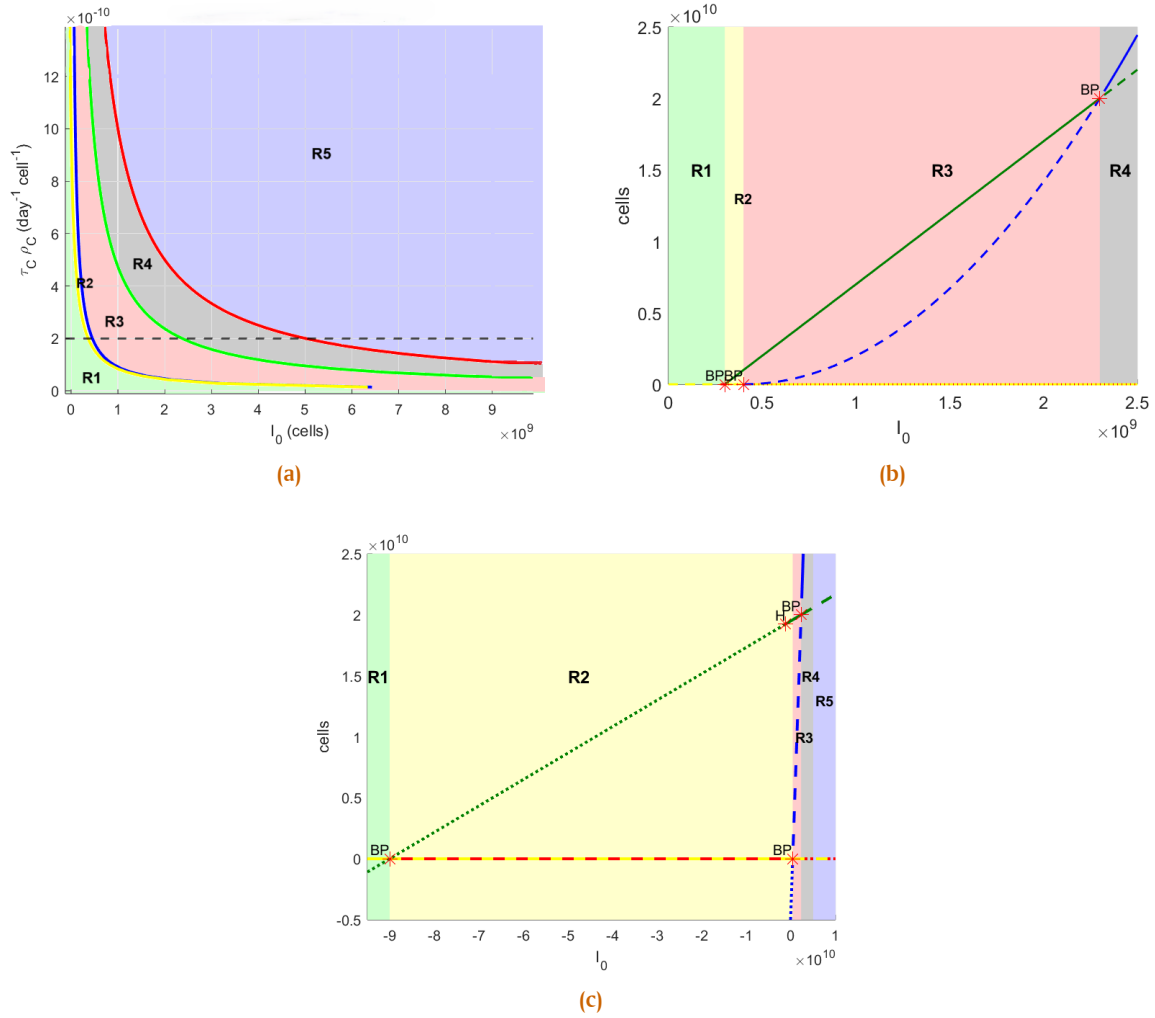

Figure 3. (a) Regions determined by the stability of the equilibria. (b) Bifurcation when I_0 varies and leukemia cell's carrying capacity $L_{\max} = 10^9$. The y-axis represents the CAR T cell population (C), while the x-axis corresponds to the initial number of progenitor B cells (I_0). (c)Bifurcation when I_0 varies and leukemia cell's carrying capacity $L_{\max} = 10^{12}$. The y-axis represents the CAR T cell population (C), while the x-axis corresponds to the initial number of progenitor B cells (I_0).

manifolds at the equilibrium point P_2 are given by $(\dim(W^s(P_2)), \dim(W^u(P_2))) = (3, 0)$.

3. The equilibrium point P_3 does not exists but is unstable. The dimension of the stable manifold is 1, while the dimension of the unstable manifold is 2. Thus, the dimensions of the manifolds at the equilibrium point P_3 are $(\dim(W^s(P_3)), \dim(W^u(P_3))) = (1, 2)$.
4. The equilibrium point P_4 does not exist because it has a negative coordinate. However, if it were to exist, it would be unstable, with a dimension of 1 for the instability manifold and a dimension of 2 for the stability manifold. Therefore, the hypothetical dimensions of the manifolds at the equilibrium point P_4 would be $(\dim(W^s(P_4)), \dim(W^u(P_4))) = (2, 1)$.

In region R_2, that is

$$I_0 \in \left(\left(\frac{1}{\rho_C \tau_C} - L_{\max} \right) \left(1 - \frac{\tau_B}{\tau_B + \tau_{I_0}} \right), \frac{1}{\rho_C \tau_C} \left(1 - \frac{\tau_B}{\tau_B + \tau_{I_0}} \right) \right).$$

The stability of each equilibrium point is as follows:

1. The equilibrium point P_1 exists and is unstable. The dimension of the instability manifold is 1, while the dimension of the stability manifold is 2. Therefore, the dimensions of the manifold at the equilibrium point P_1 are given by $(\dim(W^s(P_1)), \dim(W^u(P_1))) = (2, 1)$.
2. The equilibrium point P_2 exists and is unstable, with an instability manifold dimension of 1 and a stability manifold dimension of 2. Thus, the dimensions of the manifold at the equilibrium point P_2 are $(\dim(W^s(P_2)), \dim(W^u(P_2))) = (2, 1)$.
3. The equilibrium point P_3 does not exists and is unstable. The dimension of the stability manifold is 1, and the dimension of the instability manifold is 2. Consequently, the dimensions of the manifold at the equilibrium point P_3 are $(\dim(W^s(P_3)), \dim(W^u(P_3))) = (1, 2)$.
4. The equilibrium point P_4 exists and is asymptotically stable. Hence, the dimensions of the manifold at the equilibrium point P_4 are $(\dim(W^s(P_4)), \dim(W^u(P_4))) = (3, 0)$.

In region R_3, that is

$$I_0 \in \left(\frac{1}{\rho_C \tau_C} \left(1 - \frac{\tau_B}{\tau_B + \tau_{I_0}} \right), \frac{1}{\rho_C \tau_C} \left(1 - \frac{\tau_B}{\tau_B + \tau_{I_0}(1 + \tau_B \rho_L)} \right) \right).$$

The stability of each equilibrium point is as follows:

1. The equilibrium point P_1 exists and is unstable. The dimension of the stability manifold is 1 and the dimension of the instability manifold is 2. Hence, the dimension of the manifold at equilibrium point P_1 is $(\dim(W^s(P_1)), \dim(W^u(P_1))) = (1, 2)$.
2. The equilibrium point P_2 exists and is not stable. The dimension of the stability manifold is 2 and the dimension of the instability manifold is 1. Hence, the dimension of the manifold at equilibrium point P_2 is $(\dim(W^s(P_2)), \dim(W^u(P_2))) = (2, 1)$.
3. The equilibrium point P_3 exists and is unstable. The dimension of the stability manifold is 2. The dimension of the manifold is 1. Then the dimension of the manifold at the equilibrium point P_3 is $(\dim(W^s(P_3)), \dim(W^u(P_3))) = (2, 1)$.
4. The equilibrium point P_4 exists and is asymptotically stable so the manifold dimension at this point is $(\dim(W^s(P_4)), \dim(W^u(P_4))) = (3, 0)$.

In region R_4, that is

$$I_0 \in \left(\frac{1}{\rho_C \tau_C} \left(1 - \frac{\tau_B}{\tau_B + \tau_{I_0}(1 + \tau_B \rho_L)} \right), \frac{1}{\rho_C \tau_C} \right)$$

The stability of each equilibrium point is as follows:

1. The equilibrium point P_1 exists and is unstable. The dimension of the stability manifold is 1. The dimension of the instability manifold is 2. Hence, the dimension of the manifold at the equilibrium point P_1 is $(\dim(W^s(P_1)), \dim(W^u(P_1))) = (1, 2)$.
2. The equilibrium point P_2 exists and is unstable. The dimension of the stability manifold is 2. The dimension of the instability manifold is 1. Then the dimension of the manifold at equilibrium point P_2 is $(\dim(W^s(P_2)), \dim(W^u(P_2))) = (2, 1)$.
3. The equilibrium point P_3 exists and is asymptotically stable. Then the dimension of the manifold at the equilibrium point P_3 is $(\dim(W^s(P_3)), \dim(W^u(P_3))) = (3, 0)$.
4. The equilibrium point P_4 does not exist because there is a negative coordinate. The equilibrium point P_4 is unstable with manifold dimension 2 and manifold dimension 1. Then the manifold dimension at equilibrium point P_4 is $(\dim(W^s(P_4)), \dim(W^u(P_4))) = (2, 1)$.

In region R_5, that is $I_0 > \frac{1}{\rho_C \tau_C}$. The stability of each equilibrium point is as follows:

1. The equilibrium point P_1 exists and is unstable. The dimension of the stability manifold is 1. The dimension of the instability manifold is 2. Then the dimension of the manifold at equilibrium point P_1 is $(\dim(W^s(P_1)), \dim(W^u(P_1))) = (1, 2)$.
2. The equilibrium point P_2 exists and is unstable with a stability manifold dimension of 2 and an instability manifold dimension of 1. The manifold dimension at the equilibrium point P_2 is $(\dim(W^s(P_2)), \dim(W^u(P_2))) = (2, 1)$.
3. The equilibrium point P_3 exists and is asymptotically stable. Hence, the manifold dimension at the equilibrium P_3 is $(\dim(W^s(P_3)), \dim(W^u(P_3))) = (3, 0)$.
4. The equilibrium point P_4 does not exist because there is a negative coordinate. The equilibrium point P_4 is unstable. The dimension of the stability manifold is 2. The dimension of the manifold is 1. The dimension of the manifold at this point is $(\dim(W^s(P_4)), \dim(W^u(P_4))) = (2, 1)$.

Biologically, the five regions describe distinct outcomes of CAR T cell therapy. In Region R_1, CAR T cells provide only transient control, and leukemia eventually regrows uncontrollably, indicating treatment failure. In Region R_2 and Region R_3, the system settles into a chronic coexistence state where leukemia persists at a controlled level together with CAR T cells and B cells, reflecting partial but non-curative therapy. In contrast, Region R_4 and Region R_5 correspond to successful treatment, as leukemia is completely eradicated and long-term remission is achieved with sustained CAR T cells and B cells, representing the most favorable clinical outcome.

Using the parameter values in Table 2 and the values of the selected leukemia cell carrying capacity parameter, e.g. $L_{max} = 10^9$ and $L_{\text{max}} = 10^{12}$, there is a change in the stability of the system (1) for the parameter of the population of progenitor B cells. This indicates that the bifurcation occurs at parameter I_0.

The simulation depicted shows various equilibrium points represented by different colors: the red curve corresponds to equilibrium point P_1, the yellow curve represents P_2, the blue curve indicates P_3, and the green curve denotes P_4. Thick lines represent stable states, while dashed lines indicate unstable states. The point labeled *H* signifies a subcritical Hopf bifurcation, and *BP* marks a transcritical bifurcation point.

Figure 3b illustrate that in region R_1, the equilibrium points P_1 and P_2 are exist with the equilibrium point P_2 is stable. The equilibrium point P_2 changes to unstable when $I_0 \approx 0.36 \times 10^9$. In region R_2, the equilibrium points P_1, P_2, and P_4 are exist with the equilibrium point P_4 is stable. Region R_3, all of the equilibrium points exist and the equilibrium point P_4 is still stable. The equilibrium point P_4 changes to unstable when $I_0 \approx 2.3 \times 10^9$. This condition is a transcritical bifurcation. The equilibrium point P_4 also does not exist for region R_4 and R_5, while the equilibrium points P_1, P_2, and P_3 are exist with the equilibrium point P_3 is stable.

Biologically, the initial number of B cells progenitor strongly influences the outcome of CAR T cell therapy. When the number of B cell progenitors is very low, CAR T cells cannot persist and leukemia eventually grows back, indicating treatment failure. With a moderate number of B cell progenitors, the system reaches a state of partial control where leukemia remains but is kept at a chronic level together with CAR T cells and B cells. As the availability of progenitor B cells increases further, CAR T cells can be maintained more effectively, enabling long-term suppression and even complete elimination of leukemia. In this case, the therapy leads to stable remission, representing the most favorable clinical scenario. Overall, the figure emphasizes that sufficient support from B cell progenitors is essential for CAR T cells to survive and provide durable therapeutic benefits [22].

The following is a simulation when the carrying capacity of leukemia cells increases to $L_{\text{max}} = 10^{12}$. Since the carrying capacity of leukemia cells increases to $L_{\text{max}} = 10^{12}$, the region has a difference from the Figure 3b. Figure 3c show that in region R_1 all of the equilibrium points doesn't exist. Initially, in the region R_2 all of the equilibrium points doesn't exist. But when I_0 is zero, all of the equilibrium points are exist with stable on the equilibrium point P_4. And region R_2 also has a subcritical

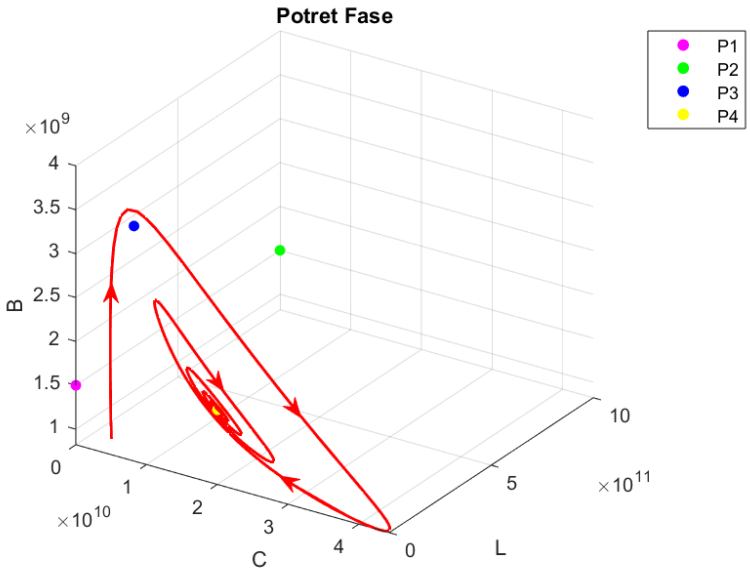

Figure 4. Phase portrait of solutions system (1) in region R_3 for $I_0 = 1.5 \times 10^9$ and $L_{\max} = 10^{12}$

hopf when $I_0 \approx -1.2 \times 10^{10}$. In the region R_3, the same of condition as the previous region. When $I_0 \approx 0.23 \times 10^{10}$, the equilibrium point P_4 changes the stability to unstable. It is a condition transcritical bifurcation. Lastly, in region R_4 and R_5, the equilibrium point P_4 doesn't exist and the equilibrium point P_3 is stable.

Biologically, illustrates that when leukemia has a very high growth capacity, CAR T therapy struggles to achieve complete remission. In region R_2, CAR T cells can initially suppress leukemia, but the system tends to fluctuate, indicating unstable control and the risk of relapse. This reflects a clinical condition where patients may experience temporary remission followed by disease resurgence. In region R_3, the situation is similar, as CAR T cells continue to coexist with leukemia cells, leading to a chronic state rather than eradication. As the system progresses to regions R_4 and R_5, leukemia grows too aggressively, and CAR T cells can no longer maintain long-term control. In this case, remission is lost and the disease stabilizes at a persistent level. Overall, this figure highlights that when leukemia has a large carrying capacity, CAR T therapy may only provide partial and temporary benefits, making long-term remission increasingly difficult to achieve [23, 24].

To further illustrate the biological consequences of the bifurcation analysis in Crefbifurkasi 2, a phase portrait is presented in Figure 4. This representation provides deeper insight into how the system evolves over time, showing the potential transition from remission to coexistence and its clinical implication as disease relapse. Figure 4 illustrates the phase portrait of the system in region R_3, where trajectories initially approach the remission equilibrium point P_3 but eventually leave it and move toward the coexistence equilibrium point P_4, forming a heteroclinic cycle. Unlike the oscillatory relapse explained by the Hopf bifurcation in Figure 8, this behavior reflects a transition between remission and coexistence states. Biologically, it suggests that remission may only be temporary: CAR T cells can suppress leukemia at first, but hidden instabilities in the immune–leukemia interaction drive the system back to coexistence, where leukemia re-emerges alongside CAR T and B cells. Clinically, this explains why some patients relapse after initial remission, highlighting that durable cure depends on the system's ability to stabilize at remission rather than cycle back to coexistence [25].

6. Conclusion

This research builds upon previous work by Serrano et al. [19], analyzed the interactions among CAR T cells, leukemia cells, and B cells and reported three equilibrium points. In contrast, this study identified four equilibria, with the additional point representing a condition where leukemia cells reach their maximum capacity at the initial stage while CAR T cells vanish and B cells persist. This difference stems from the assumption of logistic growth for leukemia cells in this study, instead of the exponential growth assumed previously. Methodologically, previous study concentrated on stability and bifurcation analysis, while this study extended the approach by incorporating numerical time-series simulations, which provided a clearer picture of transient dynamics such as temporary remission, relapse, and coexistence states.

The bifurcation outcomes also reveal important distinctions. Although both studies observed transcritical and subcritical Hopf bifurcations, this study demonstrates different patterns under varying leukemia carrying capacities and further uncovers a heteroclinic cycle that accounts for the possibility of relapse after remission. From a biological perspective, the findings highlight that B cells have a more nuanced role: beyond sustaining CAR T cell activation, an excessive number of progenitor B cells may also trigger serious clinical complications such as Cytokine Release Syndrome (CRS) and B cell aplasia. Overall, this study extends earlier results by offering deeper mathematical insights and broader clinical interpretations. For future research, the model could be refined by integrating additional biological mechanisms such as immune regulation, microenvironmental constraints, or cytokine feedback, and by validating the simulations with longitudinal clinical data. These developments would help build a

more realistic framework and support the optimization of CAR T cell therapy strategies.

Author Contributions. **Haries, E. M. D. P.**: Conceptualization, data collection, methodology, formal analysis, investigation, draft preparation, and visualization. **Abadi, A.**: Conceptualization, methodology, formal analysis, validation, discussion, review, writing, editing, and supervision.

Acknowledgement. The authors would like to thank the editors and reviewers for their careful reading, insightful criticism, and practical recommendations, which have significantly improved the quality of this manuscript.

Funding. This research received no external funding.

Conflict of interest. The authors declare no conflict of interest.

Data availability. Not applicable.

Abbreviations.

CAR T cell	:	Chimeric Antigen Receptor T cell.
B-ALL	:	B cell Acute Lymphoblastic Leukemia.
CRS	:	Cytokine Release Syndrome.

References

[1] E. N. Oretla, "Epidemiologi leukemia," https://www.alomedika.com/penyakit/hematologi/leukemia/epidemiologi, 2024, Accessed on 20 April 2025.

[2] LLS, "General blood cancers," https://www.lls.org/facts-and-statistics/facts-and-statistics-overview, 2024, Accessed on 22 April 2025.

[3] M. Zolfaghari and H. Sajedi, "A survey on automated detection and classification of acute leukemia and wbcs in microscopic blood cells," *Multimedia Tools and Applications*, vol. 81, no. 5, pp. 6723–6753, 2022. DOI:10.1007/s11042-022-12108-7

[4] A. Shah *et al.*, "Automated diagnosis of leukemia: a comprehensive review," *IEEE Access*, vol. 9, pp. 132097–132124, 2021. DOI:10.1109/ACCESS.2021.3114059

[5] N. Jiwani *et al.*, "Pattern recognition of acute lymphoblastic leukemia (all) using computational deep learning," *IEEE Access*, vol. 11, pp. 29541–29553, 2023. DOI:10.1109/ACCESS.2023.3260065

[6] A. S. Davis, A. J. Viera, and M. D. Mead, "Leukemia: an overview for primary care," *American family physician*, vol. 89, no. 9, pp. 731–738, 2014.

[7] K. Das *et al.*, "A Qualitative Analysis of Leukemia Fractional Order SICW Model," *Jambura Journal of Biomathematics (JJBM)*, vol. 5, no. 1, pp. 46–53, 2024. DOI:10.37905/jjbm.v5i1.24961

[8] C. Cobaleda and I. Sánchez-Garcia, "*Leukemia Stem Cells*." New York: Humana Press, 2021.

[9] C. K. Tebbi, "Etiology of acute leukemia: A review," *Cancers*, vol. 13, no. 9, 2021. DOI:10.3390/cancers13092256

[10] J. E. K. Ashkan Emadi, "*Acute Leukemia: An Illustrated Guide to Diagnosis and Treatment*." Demos Medical, 2018.

[11] S. Chiaretti, G. Zini, and R. Bassan, "Diagnosis and subclassification of acute lymphoblastic leukemia," *Mediterranean journal of hematology and infectious diseases*, vol. 6, no. 1, p. e2014073, 2014. DOI:10.4084/MJHID.2014.073

[12] S. P. Hunger and C. G. Mullighan, "Acute lymphoblastic leukemia in children," *New England Journal of Medicine*, vol. 373, no. 16, pp. 1541–1552, 2015. DOI:10.1056/NEJMra1400972

[13] G. Reaman and F. Smith, "*Childhood Leukemia: A Practical Handbook*." Berlin Heidelberg: Springer, 2011. DOI:10.1007/978-3-642-13781-5

[14] R. Mohanty *et al.*, "CAR T cell therapy: A new era for cancer treatment," vol. 42, no. 6, pp. 2183–2195, 2019. DOI:10.3892/or.2019.7335

[15] A. Vora, "*Childhood Acute Lymphoblastic Leukemia*." Switzerland: Springer, 2017. DOI:10.1007/978-3-319-39708-5

[16] R. C. Sterner and R. M. Sterner, "Car-t cell therapy: current limitations and potential strategies," *Blood cancer journal*, vol. 11, no. 4, p. 69, 2021. DOI:10.1038/s41408-021-00459-7

[17] M. Gabelli *et al.*, "Maintenance therapy for early loss of b-cell aplasia after anti-cd19 car t-cell therapy," *Blood advances*, vol. 8, no. 8, pp. 1959–1963, 2024. DOI:10.1182/bloodadvances.2023011168.

[18] Ã. MartÃnez-Rubio, *et al.*, "A mathematical description of the bone marrow dynamics during car t-cell therapy in b-cell childhood acute lymphoblastic leukemia," *International Journal of Molecular Sciences*, vol. 22, no. 12, 2021. DOI:10.3390/ijms22126371

[19] S. Serrano *et al.*, "Understanding the role of b cells in car t-cell therapy in leukemia through a mathematical model," *Chaos: An Interdisciplinary Journal of Nonlinear Science*, vol. 34, no. 8, 2024. DOI:10.1063/5.0206341

[20] S. E. vWillyanto *et al.*, "Comprehensive analysis of the efficacy and safety of car t-cell therapy in patients with relapsed or refractory b-cell acute lymphoblastic leukaemia: a systematic review and meta-analysis," *Annals of Medicine*, vol. 56, no. 1, p. 2349796, 2024. DOI:10.1080/07853890.2024.2349796

[21] E. Guzev *et al.*, "Validation of a mathematical model describing the dynamics of chemotherapy for chronic lymphocytic leukemia in vivo," *Cells*, vol. 11, no. 15, p. 2325, 2022. DOI:10.3390/cells11152325

[22] V. Wittibschlager *et al.*, "Car t-cell persistence correlates with improved outcome in patients with b-cell lymphoma," *International Journal of Molecular Sciences*, vol. 24, no. 6, 2023. DOI:10.3390/ijms24065688

[23] C. J. Turtle, K. A. Hay, and L. Hanafi, "Cellular dynamics after cd19 car-t cell therapy," *Nature Reviews Clinical Oncology*, vol. 19, no. 8, pp. 497–515, 2022.

[24] A. V. Hirayama and C. J. Turtle, "Mechanisms of relapse after cd19 car t-cell therapy for acute lymphoblastic leukemia and strategies to prevent it," *Blood*, vol. 141, no. 4, pp. 415–426, 2023.

[25] N. Gagelmann, F. Ayuk, and N. Kröger, "Tumor burden and car t-cell outcomes in hematologic malignancies," *Leukemia*, 2024.